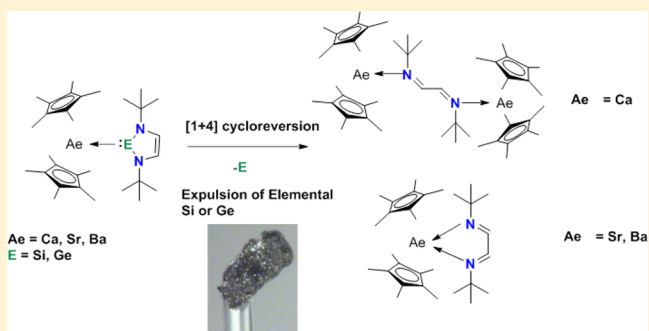


Alkaline-Earth-Metal-Induced Liberation of Rare Allotropes of Elemental Silicon and Germanium from N-Heterocyclic Metallylenes

Burgert Blom,^{*,†} Amro Said,[†] Tibor Szilvási,[‡] Prashanth W. Menezes,[†] Gengwen Tan,[†] Judith Baumgartner,[§] and Matthias Driess^{*,†}[†]Department of Chemistry: Metalorganics and Inorganic Materials, Technische Universität Berlin, Strasse des 17. Juni 135, Sekr. C2, D-10623 Berlin, Germany[‡]Department of Inorganic and Analytical Chemistry, Budapest University of Technology and Economics (BUTE), Szent Gellért tér 4, 1111 Budapest, Hungary[§]Institut für Chemie, Universität Graz, Stremayrgasse 9, 8010 Graz, Austria

Supporting Information

ABSTRACT: The synthesis and striking reactivity of the unprecedented N-heterocyclic silylene and germylene (“metallylene”) alkaline-earth metal (Ae) complexes of the type $[(\eta^5\text{-C}_5\text{Me}_5)_2\text{Ae}\leftarrow\text{E}(\text{N}^t\text{BuCH})_2]$ (3, 4, and 7–9; Ae = Ca, E = Ge 3; Ae = Sr, E = Ge 4; Ae = Sr, E = Si 7; Ae = Ba, E = Si 8; Ae = Ba, E = Ge 9) are reported. All complexes have been characterized by spectroscopic means, and their bonding situations investigated by density functional theory (DFT) methods. Single-crystal X-ray diffraction analyses of examples revealed relatively long Si–Ae and Ge–Ae distances, respectively, indicative of weak E→Ae (E = Si, Ge) dative bonds, further supported by the calculated Wiberg bond indices, which are rather low in all cases (~ 0.5). Unexpectedly, the complexes undergo facile transformation to 1,4-diazabuta-1,3-diene Ae metal complexes of the type $[(\eta^5\text{-C}_5\text{Me}_5)_2\text{Ae}(\kappa^2\text{-}\{\text{N}^t\text{Bu}=\text{CHCH}=\text{N}^t\text{Bu}\})]$ (Ae = Sr 10, Ae = Ba 11) or in the case of calcium to the dinuclear complex $[(\eta^5\text{-C}_5\text{Me}_5)_2\text{Ca}\leftarrow\text{N}(\text{tBu})=\text{CHCH}=\text{N}(\text{tBu})\rightarrow\text{Ca}(\eta^5\text{-C}_5\text{Me}_5)_2]$ (12) under concomitant liberation of elemental silicon and germanium. The formation of elemental silicon and germanium is proven by inductively coupled plasma atomic emission spectroscopy, transmission electron microscopy, selected area electron diffraction, and energy dispersive X-ray spectroscopy. Notably, the decomposition of the Si(II)→Ba complex 8 produces *allo*-silicon, a rare allotropic form of elemental silicon. Similarly, the analogous Ge(II)→Ba complex 9, upon decomposition, forms tetragonal germanium, a dense and rare allotrope of elemental germanium. The energetics of this unprecedented alkaline-earth-metal-induced liberation of elemental silicon and germanium was additionally studied by DFT methods, revealing that the transformations are pronouncedly exergonic and considerably larger for the N-heterocyclic germylene complexes than those of the corresponding silicon analogues.



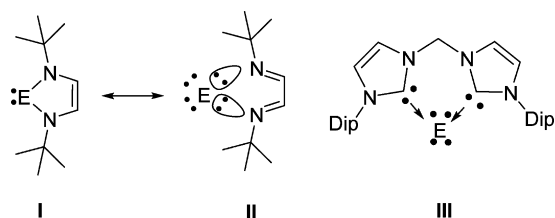
INTRODUCTION

Since the landmark discoveries of the first N-heterocyclic germylene (NHGe)¹ and the corresponding N-heterocyclic silylene (NHSi)² shortly thereafter, a plethora of d-block metal complexes bearing NHSis³ and, to a lesser extent, NHGes as supporting ligands⁴ have been reported. Both classes of complexes represent more electron-rich analogues of traditional N-heterocyclic carbene (NHC) complexes, offering pronouncedly larger σ -donor capacities and, concomitantly, different reactivities.⁵ Early investigations dating back to 1994 on first NHSi and NHGe by photoelectron spectroscopy (PES)⁶ revealed that on descent from carbon to its heavier homologues, the group 14 element atom tends to adopt zerovalent character as the HOMOs of the NHSi and NHGe become more centered on the group 14 element atom, which itself can be thought of as being chelated by a neutral 1,4-diazabuta-1,3-diene ligand and bearing two lone pairs of

electrons (resonance form II in Chart 1). This description has subsequently been largely abandoned in contemporary literature and differs substantially from the conventionally accepted bonding description (structure I in Chart 1), where the group 14 element atom is formally in the oxidation state +II, bearing only one lone pair of electrons. More recently, the existence of so-called ylidones (structure III, Chart 1) has been predicted by Frenking and co-workers⁷ and could subsequently be synthetically obtained, bearing “authentic” zerovalent group 14 atoms, with two lone pairs of electrons residing at the group 14 element atoms.⁸ The latter class of compounds offer the potential of being possible molecular precursors for zerovalent Ge and Si atoms, respectively, by ligand dissociation.

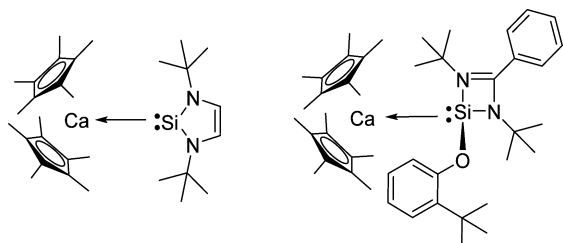
Received: July 25, 2015

Published: August 25, 2015

Chart 1. Donor–Acceptor Description of N-Heterocyclic Metallylenes I↔II and Metallylones III (E = Si, Ge)^a

^aThe resonance forms II and III bear zero-valent silicon and germanium atoms, respectively.

In recent years, our group has explored a variety of NHSi and NHGes and their capacity to coordinate to a variety of metals to afford novel complexes with a keen interest in harnessing their potential in catalysis or other transformations.⁹ As part of these efforts, we recently reported facile entry to novel s-block metal complexes bearing three- and four-coordinate NHSi ligands, namely, $[(\eta^5\text{-C}_5\text{Me}_5)_2\text{Ca}\leftarrow\text{Si}(\text{N}^t\text{BuCH})_2]$ and $[(\eta^5\text{-C}_5\text{Me}_5)_2\text{Ca}\leftarrow\text{Si}(\text{O}-\text{C}_6\text{H}_4-2\text{-}^t\text{Bu})\{(\text{N}^t\text{Bu})_2\text{CPh}\}]$, respectively (Chart 2).¹⁰ On the basis of

Chart 2. First Examples of s-Block N-Heterocyclic Silylene Complexes¹⁰

reactivity and DFT investigations it was shown that the Si:→Ca bonding interaction in both complexes is rather weak and characterized by a strong ionic component, readily seen in Bader's atoms in molecules (AIM) analysis.¹¹ Moreover, rather low Wiberg bond indices (WBIs)¹² of ~0.5 are found for both complexes, revealing only minor covalent character in the donor–acceptor Si:→Ca bond. These findings contrast strongly with the plethora of d-block NHSi complexes where

rather strong donor–acceptor interactions generally persist between the Si and metal centers and in some cases even exhibit WBIs greater than unity.¹³

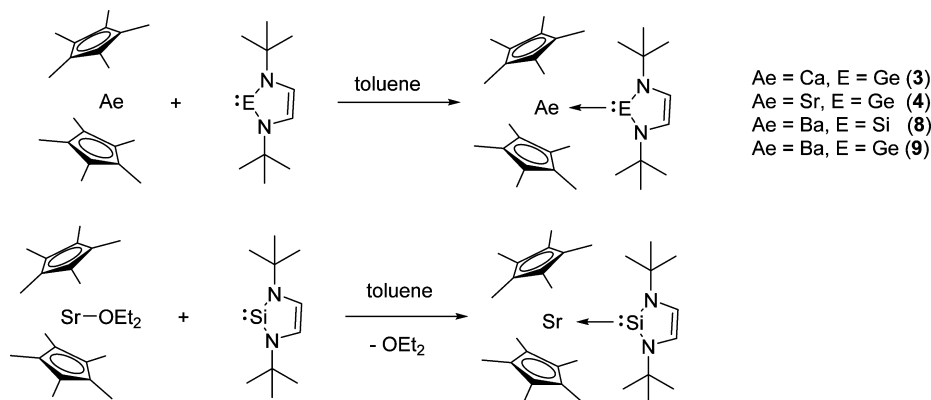
In the present report, the first examples of N-heterocyclic germylene alkaline-earth-metal (Ae) complexes (Ae = Ca, Sr, and Ba) are reported. In addition, the hitherto unprecedented NHSi complexes of Sr and Ba are also reported, with a particular focus on the trends in the bonding interaction between Si or Ge and the Ae metals. Strikingly, the coordination of the NHSi and NHGe to Ae metals induces an unprecedented facile transformation process, affording elemental silicon and germanium and the corresponding 1,4-diazabuta-1,3-diene Ae metal complexes as decomposition products. Our results confirm for the first time that NHSis and NHGes can serve as molecular precursors for elemental silicon and germanium, respectively.

RESULTS

Following a similar synthetic approach applied previously to access $[(\eta^5\text{-C}_5\text{Me}_5)_2\text{Ca}\leftarrow\text{Si}(\text{N}^t\text{BuCH})_2]$ and $[(\eta^5\text{-C}_5\text{Me}_5)_2\text{Ca}\leftarrow\text{Si}(\text{O}-\text{C}_6\text{H}_4-2\text{-}^t\text{Bu})\{(\text{N}^t\text{Bu})_2\text{CPh}\}]$, respectively,¹⁰ the reaction of $[\text{Ca}(\eta^5\text{-C}_5\text{Me}_5)_2]$ (1) with Ge($\text{N}^t\text{BuCH})_2$ (2)¹ in toluene at room temperature affords the desired $[(\eta^5\text{-C}_5\text{Me}_5)_2\text{Ca}\leftarrow\text{Ge}(\text{N}^t\text{BuCH})_2]$ adduct (3) in quantitative yields as a colorless solid (Scheme 1). Complex 3 represents the first example of an s-block NHGe complex. Extension to the heavier homologues of Ca (Sr and Ba) follows in a similar manner, and under analogous reaction conditions the complex $[(\eta^5\text{-C}_5\text{Me}_5)_2\text{Sr}\leftarrow\text{Ge}(\text{N}^t\text{BuCH})_2]$ (4) could also be isolated upon reaction of $[\text{Sr}(\eta^5\text{-C}_5\text{Me}_5)_2]$ (5)¹⁴ with NHGe 2. The reaction of the base-stabilized $(\eta^5\text{-C}_5\text{Me}_5)_2\text{Sr}(\text{OEt}_2)$ (5-OEt₂)^{15,16} complex with Si($\text{N}^t\text{BuCH})_2$ (6) affords $[(\eta^5\text{-C}_5\text{Me}_5)_2\text{Sr}\leftarrow\text{Si}(\text{N}^t\text{BuCH})_2]$ (7).

Notably, the ether donor molecule in the starting material (5-OEt₂) cannot be replaced by the NHGe but by the NHSi ligand due to the weaker σ -donor character of Ge(II) vs Si(II). Finally, the barium analogues $[(\eta^5\text{-C}_5\text{Me}_5)_2\text{Ba}\leftarrow\text{E}(\text{N}^t\text{BuCH})_2]$ (E = Si 8; E = Ge 9) could also be prepared reacting the base-free Ba($\eta^5\text{-C}_5\text{Me}_5)_2$ (5) with the NHSi 6 and NHGe 2, respectively (Scheme 1).

The high-resolution mass spectra (HR-ESI or HR-APCI) did not show the parent ($M + H^+$) peak and generally only the free NHSi or NHGe could be observed. This is very likely due to

Scheme 1. Facile Entry to the Alkaline-Earth-Metal NHSi and NHGe Complexes 3, 4, and 7–9 by Simple Coordination or Ligand Displacement Reactions

7

Table 1. Some Selected ^{29}Si and ^1H NMR Shifts in Complexes 3, 4, and 7–9 Compared with the “Free” NHGe 2 or NHSi 6

complex	^{29}Si , ppm	δ ($\text{CH}=\text{CH}$), ^1H , ppm	δ ($\text{C}(\text{CH}_3)_3$), ^1H , ppm	δ ($\text{C}_5(\text{CH}_3)_5$), ^1H , ppm
3		6.99	1.40	1.98
4		7.05	1.43	2.12
7	80.7	6.64	1.34	2.12
8	78.5 ($\Delta\nu_{1/2} = 11$ Hz)	6.74	1.40	2.06
9		7.05	1.42	2.06
NHGe 2		7.05	1.43	
NHSi 6	78.1	6.75	1.40	

the fragility of the $\text{E}:\rightarrow\text{Ae}$ coordination ($\text{E} = \text{Si}, \text{Ge}$; $\text{Ae} = \text{Ca}, \text{Sr}, \text{Ba}$), reminiscent of the calcium NHSi complexes reported earlier.¹⁰ Microanalyses were attempted on the complexes, but owing to their lability, the results were not repeatable and large variations in the C, H values were observed between measurements. Even enclosing the samples in two tin capsules did not work, likely due to their extreme sensitivity. Similar problems have been reported for alkaline-earth-metal complexes by Burns et al.¹⁸

In the multinuclear (^1H , $^{13}\text{C}\{^1\text{H}\}$, $^{29}\text{Si}\{^1\text{H}\}$) NMR spectra of all isolated complexes, their chemical shifts are only very marginally shifted from the starting materials or even identical (Table 1), indicative of a very weak coordination, akin to what was earlier observed for the complexes $[(\eta^5\text{-C}_5\text{Me}_5)_2\text{Ca}\leftarrow:\text{Si}(\text{N}^t\text{BuCH})_2]$ and $[(\eta^5\text{-C}_5\text{Me}_5)_2\text{Ca}\leftarrow:\text{Si}(\text{O}-\text{C}_6\text{H}_4\text{-}2\text{-}^t\text{Bu})\{(\text{N}^t\text{Bu})_2\text{CPh}\}]$, respectively.¹⁰ Accordingly, the ^{29}Si NMR chemical shift of the Sr complex 7 occurs at roughly the same value as that of its calcium analogue reported earlier, indicating no or a very slow exchange process on the NMR time scale of the measurement. In contrast, the ^{29}Si NMR shift of the barium complex 8 is broadened ($\Delta\nu_{1/2} = 11$ Hz) and at roughly at the same chemical shift position of the free NHSi , suggestive of a detectable exchange process on the time scale of the ^{29}Si NMR measurement.¹⁷ This situation is similar to what was observed for a series of $[(\eta^5\text{-C}_5\text{Me}_5)_2\text{Ae}\leftarrow:\text{PEt}_3]$ complexes ($\text{Ae} = \text{Ca}, \text{Sr}, \text{Ba}$) reported by Burns et al.,¹⁸ where a detectable exchange process was found for both Sr and Ba, suggestive of slightly weaker coordination in solution, compared with its calcium analogue.

In order to further probe this exchange phenomenon, NMR-scale experiments were conducted where two equivalents of the NHSi were added to one equivalent of the $[(\eta^5\text{-C}_5\text{Me}_5)_2\text{Ae}]$ ($\text{Ae} = \text{Ca}, \text{Ba}$) or $[(\eta^5\text{-C}_5\text{Me}_5)_2\text{Sr}(\text{OEt}_2)]$, respectively, and ^1H and ^{29}Si spectra were recorded at room temperature. In all cases, in the ^1H NMR spectra, only one set of sharp resonance signals was detected, despite the presence of two equivalents of the NHSi , roughly in between the resonance signals of the free NHSi and that of the isolated complex, signifying rapid exchange (see Supporting Information). Moreover, in the ^{29}Si NMR spectra only one resonance signal was observed in all three cases, also demonstrating exchange dynamics in solution. These results collectively and conclusively show that the coordination of the NHE ($\text{E} = \text{Si}, \text{Ge}$) to the alkaline-earth metal is labile and has the propensity to readily undergo facile exchange in solution.

Obtaining crystals suitable for single-crystal X-ray structural investigations of the complexes proved very difficult. In the case of 3 suitable colorless crystals could be obtained, and the structure solution revealed two independent molecules of 3 in the asymmetric unit (see Figure S13, Supporting Information). This data set was however of moderate precision (R_1 all data = 0.3195; wR_2 all data = 0.3534), so another crystallization of

complex 3 over a longer period (>1 week) was carried out. This procedure however afforded red crystals with a data set of higher precision, but contained two molecules in the asymmetric unit, namely, complex 3 and a decomposition product: the dinuclear 1,4-diaza-1,3-butadiene complex $[(\eta^5\text{-C}_5\text{Me}_5)_2\text{Ca}\leftarrow:\text{N}^t\text{Bu}=\text{CHCH}=\text{N}^t\text{Bu}:\rightarrow\text{Ca}(\eta^5\text{-C}_5\text{Me}_5)_2]$ (12) (Figures 1 and 2).

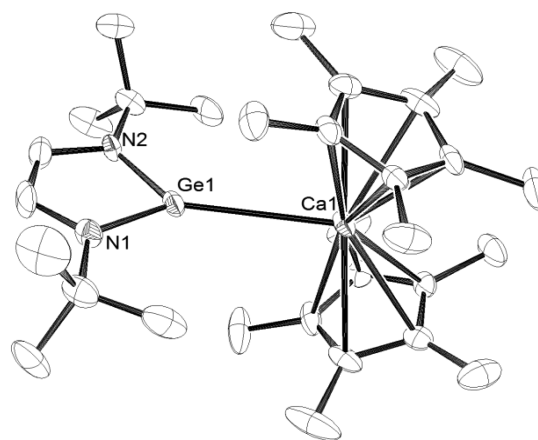


Figure 1. ORTEP representation of 3 in the solid state as one of the molecules in the asymmetric unit alongside the decomposition product 12. Thermal ellipsoids are set at the 50% probability level; H atoms are omitted for clarity. Selected distances [Å]: $\text{Ca}(1)\text{-Ge}(1)$ 3.1174(11), $\text{Ge}(1)\text{-N}(1)$ 1.844(4), $\text{Ge}(1)\text{-N}(2)$ 1.843(4). Selected angles [deg]: $\text{N}(1)\text{-Ge}(1)\text{-Ca}(1)$ 134.76(15), $\text{N}(2)\text{-Ge}(1)\text{-Ca}(1)$ 138.66(11), $\text{N}(2)\text{-Ge}(1)\text{-N}(1)$ 85.51(18).

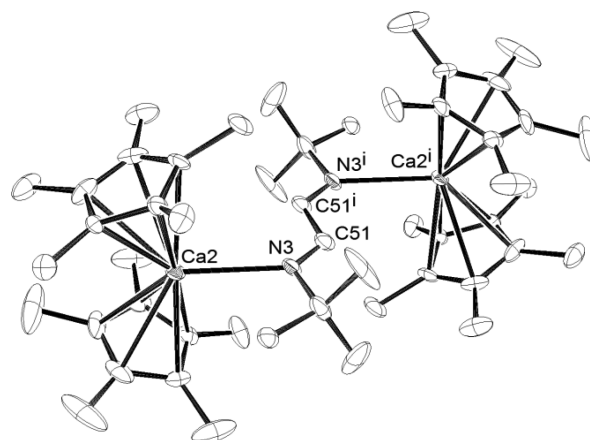


Figure 2. ORTEP representation of 12 in the solid state. Thermal ellipsoids are set at the 50% probability level; H atoms omitted for clarity. Selected bond lengths [Å]: $\text{Ca}(2)\text{-N}(3)$ 2.610(4), $\text{N}(3)\text{-C}(51)$ 1.262(7), $\text{C}(51)\text{-C}(51^i)$ 1.471(9).

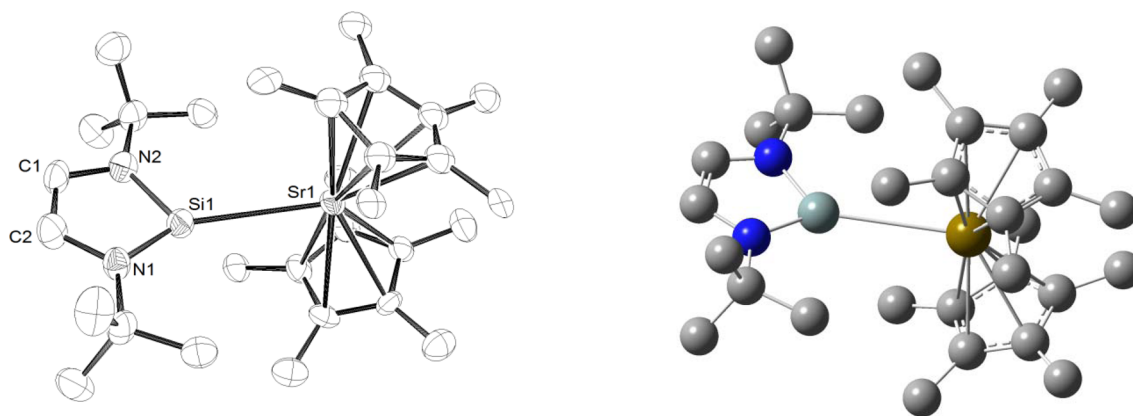


Figure 3. ORTEP representation of **7** in the solid state (left). Thermal ellipsoids are set at the 50% probability level; H atoms omitted for clarity. Optimized structure of complex **7** derived by DFT methods B97-D/def2-TZVP[C,N,H:6-31G(d)]. Calculated Si–Sr bond length: 3.272 Å (gold = Sr; cyan = Si; dark blue = N; gray = C.).

Complex **3** is the first example of an s-block NHGe complex, which is structurally analogous with the silicon analogue reported earlier.¹⁰ The complex features tilted Cp* rings with the NHGe ligand occupying a free coordination site. The Ge–Ca distance of 3.1174(11) Å is rather long, akin to what was observed for the Si analogue and longer than the values observed for existing calcium germanide complexes, which are exceptionally rare in their own right.¹⁹ The complex [Ca(thf)₃{Ge(TMS)₃}₂] (TMS = trimethylsilyl), by Teng and Ruhlandt-Senge, for example, features an average Ca–Ge distance of 3.022 Å. The notably long bond length supports the notion that the bonding situation between Ge and Ca is likely a very weak donor–acceptor interaction. The Ge center in **3** is almost trigonal planar with the sum of bond angles around the Ge atom of 358.93°.

As mentioned above the asymmetric unit also contained the decomposition product [(η⁵-C₅Me₅)₂Ca←:N(^tBu)=CHCH=(^tBu)N→Ca(η⁵-C₅Me₅)₂], **12**. Remarkably, the mode of decomposition from **3** to **12** clearly involves unprecedented liberation of elemental germanium (see below for detailed discussion). The structure of **12** is shown in Figure 2.

Compound **12** possesses a mirror plane between C51 and C51' in the asymmetric unit. The N3–C51 distance is 1.262(7) Å and, hence, represents a double bond. According to the metric parameters, **12** is a dicalcium(II) complex with a bridging neutral 1,4-diazabuta-1,3-diene ligand. The Ca–N bond length is comparable to, albeit slightly longer than, the related *ansa*-metallocene complex from Edlmann and co-workers, [Ca{Me₄C₂-(η⁵-C₅H₄)}(κ²-{N^tBu=CHCH=N^tBu})]: Ca–N = 2.503(6) and 2.564(6) Å, respectively.²⁰ Compound **12** was synthesized independently by the reaction of **1** with the respective 1,4-diazabuta-1,3-diene ligand, ^tBuN=C(H)–C(H)=N^tBu, in the molar ratio of 2:1 (see below).

For complex **7**, substantial difficulties arose in trying to obtain suitable crystals for a single-crystal X-ray diffraction analysis. Because the crystal quality of **7** turned out to be moderate and led only to a medium precision of metric parameters, DFT calculations at the B97-D/def2-TZVP-[C,N,H:6-31G(d)] level of theory were performed (see below). The connectivity of **3** as determined by an X-ray diffraction analysis is in accordance with the results by DFT calculations (Figure 3). The calculated Si–Sr bond length is 3.272 Å, which again falls outside the sum of the single-bond

covalent radii of both elements (Sr = 0.185 Å; Si = 0.116 Å),²² indicative of a weak donor–acceptor interaction. To our knowledge, only two examples of molecular complexes bearing Sr–Si bonds were reported by Teng and Ruhlandt-Senge: [Sr(thf)₃{Si(TMS)₃}₂], where the average Sr–Si bond length is 3.196 Å, and [Sr(tmeda)(thf){Si(TMS)₃}₂] (tmeda = N,N,N',N'-tetramethylethylenediamine), which features an average Sr–Si bond length of 3.223 Å.²¹

In close analogy with the NHGe→Ca complex **3**, complex **7** also undergoes repeatable decomposition to a 1,4-diazabuta-1,3-diene Sr(II) complex upon prolonged standing in solution (>1 week) to give [(η⁵-C₅Me₅)₂Sr(κ²-{N^tBu=CHCH=N^tBu})], **10**. This corresponds with concomitant extrusion of elemental silicon, akin to what was observed for **3**, and highlights the apparently similar lability of complexes **3** and **7**. In contrast to the decomposition product of **3**, which is dinuclear, complex **10** is mononuclear and bears only one chelating 1,4-diazabuta-1,3-diene ligand in κ²-fashion. The probable reason for the difference in coordination mode of the ligand is the increased ion radius of Sr(II) vs Ca(II),²² which facilitates κ²-coordination toward Sr(II). The molecular structure of **10** is shown in Figure 4. Noteworthy is the rather acute bite angle of the chelating C₂N₂ ligand (62.36°). The Sr–

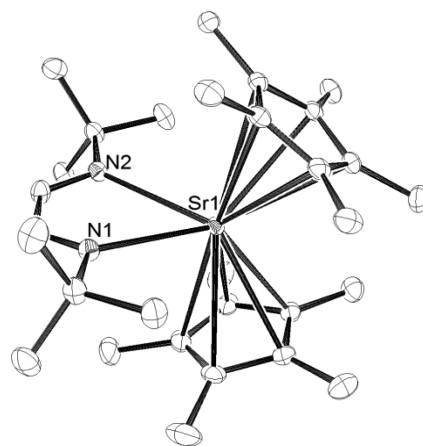


Figure 4. ORTEP representation of **10**. Thermal ellipsoids are set at the 50% probability level; H atoms are omitted for clarity. Selected bond lengths [Å]: Sr(1)–N(1) 2.7451(13), Sr(1)–N(2) 2.7538(13). Selected bond angle [deg]: N(1)–Sr(1)–N(2) 62.36(4).

Scheme 2. Direct Syntheses of 10–12

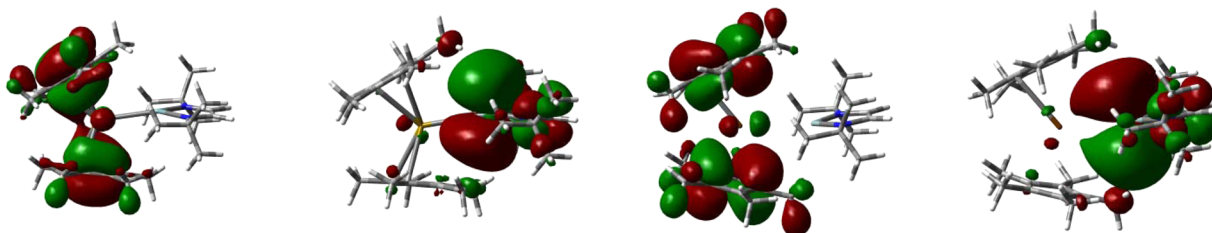
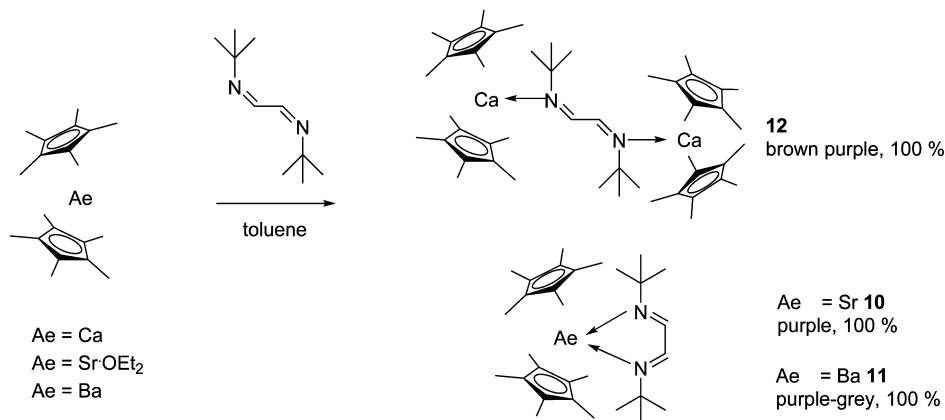


Figure 5. Boundary surface plots of the frontier orbitals (from left to right) in complex 4: (HOMO, -3.64 eV); (LUMO, -1.69 eV) and 8: (HOMO, -3.53 eV); (LUMO, -1.56 eV). Complexes were optimized at the B97-D/def2-TZVP[C,N,H:6-31G(d)] level of theory.

N1 and Sr–N2 bond lengths (2.7451(13), 2.7538(13) Å, respectively) are slightly longer in comparison to the only existing complex with which a meaningful comparison can be made: $\text{Sr}(\eta^5\text{-C}_5\text{Me}_5)_2(\kappa^2\text{-}\{\text{Bipy}\})$ (Bipy = bipyridine), where Sr–N = 2.624(3) and 2.676(3) Å, respectively.²³

Attempts at growing crystals of the $\text{NHGe} \rightarrow \text{Sr}$ complex 4 were unsuccessful and in each instance afforded exclusively compound 10 along with formation of elemental germanium. Similarly, for the barium complexes 8 and 9, we were unable to obtain suitable crystals for a single-crystal X-ray diffraction analysis. In both instances, even growing crystals at -78 °C, we obtained single crystals of the Ba analogue of 10, $[(\eta^5\text{-C}_5\text{Me}_5)_2\text{Ba}(\kappa^2\text{-}\{\text{N}^t\text{Bu}=\text{CHCH}=\text{N}^t\text{Bu}\})]$; its connectivity could be proven by X-ray diffraction analysis, but the poor crystal quality precludes a discussion of metric parameters.

These results collectively show that the $\text{NHE} \rightarrow \text{Ae}$ complexes (Ae = Ca, Sr, Ba) are thermodynamically unstable and prone to decomposition, which is in line with results from DFT (density functional theory) calculations (see below).

All of the respective 1,4-diazabuta-1,3-diene Ae decomposition complexes 10–12 could readily be synthesized by direct reactions of 1,4-diazabuta-1,3-diene ${}^t\text{BuN}=\text{CHCH}=\text{N}^t\text{Bu}$ with the respective Cp^*_2Ae (Ae = Ca, Sr, Ba) precursors. While the reaction of ${}^t\text{BuN}=\text{CHCH}=\text{N}^t\text{Bu}$ with $[(\eta^5\text{-C}_5\text{Me}_5)_2\text{Ca}]$ in the molar ratio of 1:1 afforded a mixture of products, the reaction in the ratio of 1:2 cleanly afforded 12. This result fits with the decomposition mode of $[(\eta^5\text{-C}_5\text{Me}_5)_2\text{Ca} \leftarrow \cdot\text{Ge}(\text{N}^t\text{BuCH})_2]$ (3) to give merely 12. In contrast, the reactions of ${}^t\text{BuN}=\text{CHCH}=\text{N}^t\text{Bu}$ with one molar equivalent of 5-OEt_2 afforded complex 11 selectively, with concomitant OEt_2 elimination, and in analogy, the reaction of ${}^t\text{BuN}=\text{CHCH}=\text{N}^t\text{Bu}$ with $[(\eta^5\text{-C}_5\text{Me}_5)_2\text{Ba}]$ in the molar ratio of 1:1 yielded complex 11 quantitatively (Scheme 2).

DFT analyses at the B97-D/def2-TZVP[C,N,H:6-31G(d)] level of theory were carried out for complexes 3, 4, 7, 8, and 9 in order to gain insights into the bonding situation between the group 14 element and the alkaline-earth metal; in addition, the silicon and germanium liberation processes with corresponding formation of the respective 1,4-diazabuta-1,3-diene Ae complexes were investigated computationally.

In the $\text{NHE} \rightarrow \text{Ae}$ complexes (3, 4, 7–9) the HOMO is localized on the Cp^* rings, with some delocalization over the metal center (Figure 5 and Supporting Information). The LUMO is in all cases located on the coordinated metallylene ligand. This picture resembles the situation of the calcium complexes studied previously.¹⁰

A donor–acceptor interaction from the divalent group 14 site to the Ae cation is clearly visible in each complex and represented by the HOMO–5 of complex 3, where some orbital contribution from the calcium center is also involved (Figure 6 and Supporting Information). Surprisingly, the absolute energies of the HOMO–5 are very similar across

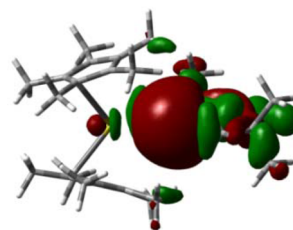


Figure 6. Boundary surface plot of the HOMO–5 of complex 3 showing the donor–acceptor interaction between Ge and Ca. For complexes 4, 7, 8, and 9 a very similar picture emerges (see Supporting Information); the complexes were optimized at the B97-D/def2-TZVP[C,N,H:6-31G(d)] level of theory.

all the complexes, and Table 2 provides the computed energies of the HOMOs–5 and the calculated E:→Ae (E = Si, Ge; Ae = Ca, Sr, Ba) distances.

Table 2. Energies of the HOMOs–5 and Calculated E:→Ae Distances (in Å) for 3, 4, 7, 8, and 9

complex	energy HOMO–5 (eV)	d(E:→Ae) calculated	d(E:→Ae) by X-ray analysis
Ge:→Ca (3)	–6.21	3.166	3.1174(11)
Ge:→Sr (4)	–6.36	3.319	
Si:→Sr (7)	–6.06	3.272	3.224(3)
Si:→Ba (8)	–6.04	3.491	
Ge:→Ba (9)	–6.36	3.565	

The NBO analyses of the E:→Ca (E = Si, Ge) bonds revealed high s-character with a heavily polarized bonding situation toward the group 14 atom (Table 3). In the case of

Table 3. NBO Analyses of the σ -Donation from E(II):→Ae in the Complexes 3, 4, and 7–9^a

		atom	polarization	s-character	p-character	d-character
Ca–Ge (3)	σ -bond	Ca	16.50%	14.24%	35.63%	50.13%
		Ge	83.50%	59.82%	40.06%	0.10%
Sr–Si (7)	lone pair	Si		74.25%	25.69%	0.05%
		Ge		82.43%	17.52%	0.05%
Ba–Si (8)	lone pair	Si		74.59%	25.36%	0.04%
		Ge		82.72%	17.25%	0.03%
NHGe	lone pair	Si		78.95%	21.01%	0.04%
		Ge		86.40%	13.58%	0.02%

^aNote that for complexes 4 and 7–9 the NBO analysis dissects the bond into lone pairs on the E(II) centers and empty orbitals on Ae since the bonds are very polarized (>90% E, <10% Ae).

the Sr and Ba complexes, the bond is polarized in such a way that the NBO analysis dissects it into a donor lone pair localized on the group 14 atom and a vacant acceptor orbital at the Ae center. This result shows that on descent from calcium to its heavier homologues, the donor–acceptor strength of the bonds decreases, a result that is also shown by a subtle decrease in the WBI (see below).

Inspection of Table 4 readily shows that for all complexes a rather low WBI exists for the donor–acceptor E:→Ae interaction. Remarkably, the WBIs of the calcium complexes are somewhat higher than the corresponding Sr and Ba

Table 4. Wiberg Bond Index (WBI) and Mayer Bond Order (MBO) of the E:→Ae Interactions and Charges of the Ae Elements (Ae = Ca, Sr, Ba) and E(II) Centers (E = Si, Ge) in the Complexes 3, 4, and 7–9

compound	WBI	MBO	charge of Ae element	charge of E
Ge:→Ca (3)	0.53	0.16	+0.84	+1.05
Si:→Sr (7)	0.44	0.18	+1.14	+1.03
Ge:→Sr (4)	0.41	0.14	+1.15	+0.92
Si:→Ba (8)	0.44	0.17	+1.11	+1.03
Ge:→Ba (9)	0.42	0.16	+1.09	+0.92

analogues. Noteworthy is that within each couple (NHSi vs NHGe Ca, Sr, and Ba complexes, respectively) the NHSi complex exhibits a slightly higher WBI compared to the NHGe analogue, which is a consequence of the enhanced σ -donor ability of Si(II) vs Ge(II), resulting in a slightly stronger Si:→Ae interaction.

According to weak E:→Ae bonding interactions, the calculated bond dissociation energies (Table 5) are very low

Table 5. Bond Dissociation Energies (BDE) of Complexes 3, 4, and 7–9 into NHSi/NHGe and $[(\eta^5\text{-C}_5\text{Me}_5)_2]\text{Ae}$ (in kcal mol^{–1})

complex	BDE
Ge:→Ca (3)	19.7
Si:→Sr (7)	22.9
Ge:→Sr (4)	20.8
Si:→Ba (8)	24.4
Ge:→Ba (9)	21.7

for all complexes (19.7–22.9 kcal mol^{–1}). Again, for each Ae (Ca, Sr, Ba) complex, the NHSi exhibits a slightly larger BDE compared with the respective NHGe analogue. It is of interest to note that while there appears to be a decrease in the covalency on descending from Ca to Ba, the BDE on average increases. This might be due to a preponderance of increased ionic contributions, which result in a more stable bonding interaction.

Most striking, however, is the propensity of complexes 3, 4, and 7–9 to undergo a different decomposition process induced by the Ae metal with concomitant liberation of elemental silicon and germanium and the formation of the respective 1,4-diazabuta-1,3-diene Ae complexes 10–12 (Scheme 3). The liberation of neutral group 14 elements from metallocenes has merely been reported for N-heterocyclic stannylenes and germlylenes by indirect means,²⁴ but to date no such facile process is reported for NHSi. To exclude the possibility that the decomposition is perhaps triggered by the presence of trace amounts of O₂ or H₂O, control experiments were conducted.²⁵

The liberation of Si(0) and Ge(0) was calculated for all the complexes. In all cases it was found that the main driving force of the decomposition is the formation of crystalline silicon and germanium (Table 6). In particular, on descending from Ca to Ba, the extrusion process becomes considerably more thermodynamically favorable, which explains the facile formation of 10–12. Moreover, the free-energy change ΔG for the NHGe complexes is considerably more negative than those of the corresponding NHSi complexes, which is likely due to the increased propensity of the heavier group 14 elements to undergo this [1+4] cycloreversion process²⁴ caused by the zerovalent nature of a heavier group 14 atom in such metallocenes.⁶ Notably, the liberation process of silicon and germanium from the “free” NHSi (–2.4 kcal·mol^{–1}) and NHGe (–15.5 kcal·mol^{–1}) is considerably less thermodynamically favored, respectively. This underlines the fact that the process is facilitated by coordination of the metallocene ligand to the Ae center and likely driven by the high stability of the resulting 1,4-diazabuta-1,3-diene Ae complexes.

Furthermore, we were curious about the nature of elemental silicon and germanium produced from the molecular precursors 8 and 9, respectively. The thermal decomposition of 8 afforded lustrous, large, grayish-black samples of elemental silicon (Figures S6–S9 in the Supporting Information), whereas 9

Scheme 3. Decomposition of 3, 4, and 7–9 to Afford the Corresponding 1,4-Diazabuta-1,3-diene Ae Complexes 10–12 with Concomitant Liberation of Elemental Silicon and Germanium

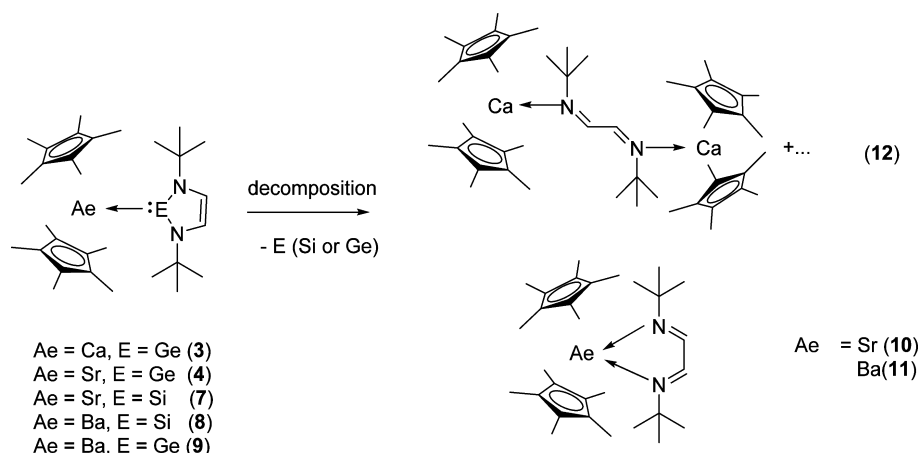


Table 6. Calculated Free Energy Change (ΔG in kcal mol⁻¹) for the Facile Decomposition of Complexes 3, 4, and 7–9 to the Corresponding 1,4-Diazabuta-1,3-diene Ae Complexes 10–12 and Elemental Silicon and Germanium (Si(0) and Ge(0))

decomposition process	ΔG
$[(\eta^5\text{-C}_5\text{Me}_5)_2\text{Ca} \leftarrow \text{:Si}(\text{N}^t\text{BuCH}_2)_2] \rightarrow 12 + \text{Si}(0)$	-23.7
$3 \rightarrow 12 + \text{Ge}(0)$	-36.7
$4 \rightarrow 10 + \text{Ge}(0)$	-26.7
$7 \rightarrow 10 + \text{Si}(0)$	-40.4
$8 \rightarrow 11 + \text{Si}(0)$	-35.4
$9 \rightarrow 11 + \text{Ge}(0)$	-48.7
$\text{:Si}(\text{N}^t\text{BuCH}_2)_2 \rightarrow \text{Si}(0) + {}^t\text{BuN}=\text{CHCH}=\text{N}^t\text{Bu}$	-2.4
$\text{:Ge}(\text{N}^t\text{BuCH}_2)_2 \rightarrow \text{Ge}(0) + {}^t\text{BuN}=\text{CHCH}=\text{N}^t\text{Bu}$	-15.5

produced small particles of elemental germanium (Figure S10 in the Supporting Information), as confirmed by inductively coupled plasma atomic emission spectroscopy (ICP-AES), transmission electron microscopy (TEM), selected area

electron diffraction (SAED), and energy dispersive X-ray spectroscopy (EDX) (Figures S11 and S12 in the Supporting Information).

The samples turned out to be only partially crystalline, as shown by X-ray diffraction analyses; unfortunately, due to weak reflections, the determination of the unit cell was not possible. However, an SAED investigation of the silicon samples yielded from 8 could be carried out, and from the unique $d(hkl)$ values, the data correspond to the rare metastable silicon allotrope named *allo*-silicon (Figure 7, JCPDS 41-1111).²⁶ The *allo*-Si form was first reported as a result of the decomposition of the silicon-rich silicide Li_3NaSi_6 in a solution of benzophenone in dry THF over several weeks.²⁶ Since then, exhaustive strategies have been applied to determine its structure by a combination of experimental and quantum chemical methods, but the structure still remains elusive.^{26,27} Although a structural model for *allo*-Si has been proposed, it has escaped experimental elucidation.²⁸

Remarkably, the analysis of the SAED pattern on elemental germanium yielded from 9 revealed that the dense form of

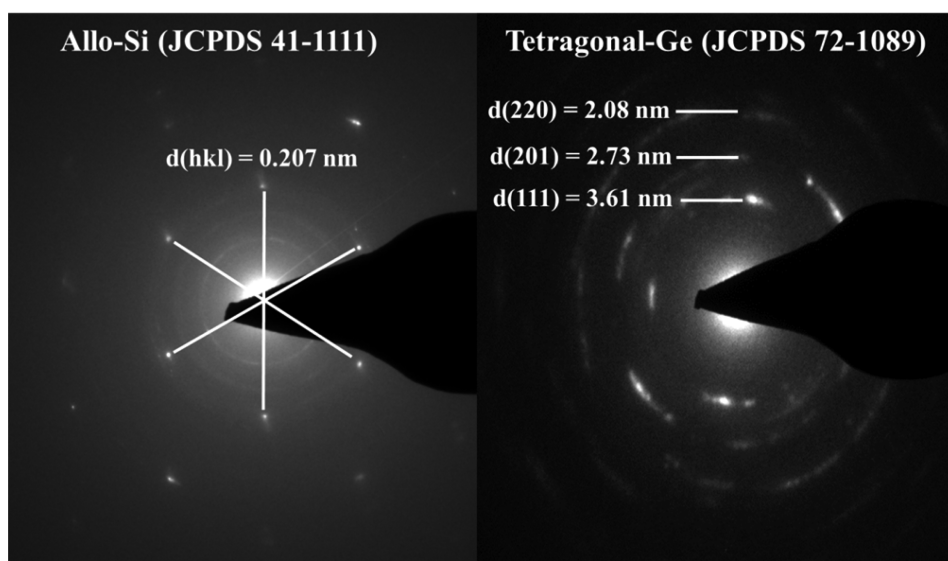


Figure 7. Selected area electron diffraction (SAED) pattern on elemental silicon and germanium samples synthesized from the molecular precursors 8 (formation of *allo*-silicon, left) and 9 (tetragonal-germanium, right), respectively. The $d(hkl)$ values clearly indicate the formation of *allo*-silicon, a rare allotrope of silicon and a dense form of solid tetragonal germanium (see also the Supporting Information).

tetragonal-germanium (JCPDS 72-1089, Figure 7), also known as Ge-III or an ST-12 structure, was formed. The latter allotrope represents a somewhat rare metastable form of germanium, which was first reported in 1963 by compressing diamond-like cubic germanium at high pressures and reducing the pressure back to atmospheric.²⁹ Theoretical calculations predicted that this Ge allotrope is a semiconductor with a direct gap of only 1.47 eV³⁰ and, therefore, has been considered very attractive for device applications, especially in the area of optoelectronics and photovoltaics. Given the potential use of this allotrope, its facile preparation reported here is of obvious interest.

SUMMARY AND CONCLUSIONS

The first complete series of N-heterocyclic germylene and N-heterocyclic silylene alkaline-earth-metal complexes have been prepared and characterized spectroscopically, in selected cases by X-ray diffraction analysis, and investigated by DFT methods. All complexes feature very weak donor–acceptor interactions with limited covalency in the E→Ae bond (E = Si, Ge; Ae = Ca, Sr, Ba). The complexes are thermodynamically unstable and prone to decomposition, affording in the case of calcium the dinuclear complex $[(\eta^5\text{-C}_5\text{Me}_5)_2\text{Ca} \leftarrow \text{N}^t\text{Bu}=\text{CHCH}=\text{BuN} \rightarrow \text{Ca}(\eta^5\text{-C}_5\text{Me}_5)_2]$ (12) and in the cases of Sr and Ba the chelate 1,4-diazabuta-1,3-diene complexes $[(\eta^5\text{-C}_5\text{Me}_5)_2\text{Ae}(\kappa^2\text{-}\{\text{N}^t\text{Bu}=\text{CHCH}=\text{N}^t\text{Bu}\})]$ (Ae = Sr 10 and Ae = Ba 11). This decomposition process is accompanied by the unexpected facile liberation of Si(0) and Ge(0), in accordance with what was proposed more than 20 years ago on the N-heterocyclic metallylenes based on photoelectron spectroscopy.⁶ Most notably, the thermal decomposition of 8 and 9 led to rare allotropes of the respective elements: *allo*-silicon and tetragonal germanium, a dense form of solid germanium, could be isolated and characterized by several methods. The results presented here highlight new possibilities in the generation of rare and otherwise inaccessible allotropes of silicon and germanium from readily accessible molecular precursors under facile reaction conditions. Not only due to the superior electronic properties of elemental silicon and germanium in technological applications but also from a fundamental point of view, the route highlighted in this report is of general interest.^{31,32} We are currently investigating how different reaction conditions and modifications in pressure might enable access to other hitherto unknown allotropes of silicon and germanium.

ASSOCIATED CONTENT

Supporting Information

The Supporting Information is available free of charge on the ACS Publications website at DOI: 10.1021/acs.inorgchem.5b01643.

Experimental details and procedures and details on X-ray crystal structure analyses, selected NMR spectra, additional details on the characterization of elemental silicon and germanium, as well as the Cartesian coordinate NBO analyses, optimized structures, and additional MOs of all complexes (PDF)

Crystallographic data for complexes 3 and 12 (CIF)

Crystallographic data for complex 5 (CIF)

Crystallographic data for complex 7 (CIF)

Crystallographic data for complex 10 (CIF)

AUTHOR INFORMATION

Corresponding Authors

*E-mail: burgert.blom@tu-berlin.de.

*E-mail: matthias.driess@tu-berlin.de.

Notes

The authors declare no competing financial interest.

ACKNOWLEDGMENTS

We are grateful to the Cluster of Excellence “UniCat” (sponsored by the Deutsche Forschungsgemeinschaft and administered by the TU Berlin) for financial support of this research and Dr. C. Göbel for TEM measurements.

REFERENCES

- Herrmann, W. A.; Denk, M.; Behm, J.; Scherer, W.; Klingan, F. – R.; Bock, H.; Solouki, B.; Wagner, M. *Angew. Chem., Int. Ed. Engl.* **1992**, *31*, 1485.
- Denk, M.; Lennon, R.; Hayashi, R.; West, R.; Belyakov, A. V.; Verne, H. P.; Haaland, A.; Wagner, M.; Metzler, N. *J. Am. Chem. Soc.* **1994**, *116*, 2691.
- For recent reviews see: (a) Blom, B.; Gallego, D.; Driess, M. *Inorg. Chem. Front.* **2014**, *1*, 134. (b) Blom, B.; Stoelzel, M.; Driess, M. *Chem. - Eur. J.* **2013**, *19*, 40. (c) Blom, B.; Driess, M. *Struct. Bonding (Berlin)* **2014**, *156*, 85.
- See as selected examples: (a) Jones, C.; Rose, R. P.; Stasch, A. *Dalton Trans.* **2008**, 2871. (b) Matioszek, D.; Katir, N.; Saffon, N.; Castel, A. *Organometallics* **2010**, *29*, 3039. (c) Cabeza, J. A.; García-Álvarez, P.; Pérez-Carreño, E.; Polo, D. *Inorg. Chem.* **2014**, *53*, 8735. (d) Gallego, D.; Inoue, S.; Blom, B.; Driess, M. *Organometallics* **2014**, *33*, 6885. (e) Matioszek, D.; Saffon, N.; Sotiropoulos, J.-M.; Miqueu, K.; Castel, A.; Escudí, J. *Inorg. Chem.* **2012**, *51*, 11716. (f) Cabeza, J. A.; García-Álvarez, P.; Polo, D. *Dalton. Trans.* **2013**, *42*, 1329. (g) Cabeza, J. A.; García-Álvarez, P.; Pérez-Carreño, E.; Polo, D. *Chem. - Eur. J.* **2014**, *20*, 8654. (h) Nagendran, S.; Sen, S. S.; Roesky, H. W.; Koley, D.; Grubmüller, H.; Pal, A.; Herbst-Irmer, R. *Organometallics* **2008**, *27*, 5459.
- See as leading references of NHC compounds and their relevance: (a) Herrmann, W. A. *Angew. Chem., Int. Ed.* **2002**, *41*, 1290. (b) Nair, V.; Bindu, S.; Sreekumar, V. *Angew. Chem., Int. Ed.* **2004**, *43*, 5130. (c) Lin, J. C. Y.; Huang, R. T. W.; Lee, C. S.; Bhattacharyya, A.; Hwang, W. S.; Lin, I. J. B. *Chem. Rev.* **2009**, *109*, 3561. (d) Diez-González, S.; Marion, N.; Nolan, S. P. *Chem. Rev.* **2009**, *109*, 3612. (e) Poyatos, M.; Mata, J. A.; Peris, E. *Chem. Rev.* **2009**, *109*, 3677. (f) Kantchev, E. A. B.; O'Brien, C. J.; Organ, M. G. *Angew. Chem., Int. Ed.* **2007**, *46*, 2768. (g) *N-Heterocyclic Carbenes in Synthesis*; Nolan, S. P., Ed.; Wiley-VCH Verlag GmbH & Co. KGaA: Weinheim, Germany, 2006.
- Arduengo, A. J., III; Bock, H.; Chen, H.; Denk, M.; Dixon, D. A.; Green, J. C.; Herrmann, W. A.; Jones, N. L.; Wagner, M.; West, R. J. *Am. Chem. Soc.* **1994**, *116*, 6641.
- (a) Tonner, R.; Frenking, G. *Angew. Chem., Int. Ed.* **2007**, *46*, 8695. (b) Tonner, R.; Frenking, G. *Chem. - Eur. J.* **2008**, *14*, 3260. (c) Tonner, R.; Frenking, G. *Chem. - Eur. J.* **2008**, *14*, 3273. (d) Tonner, R.; Frenking, G. *Pure Appl. Chem.* **2009**, *81*, 597. (e) Takagi, N.; Shimizu, T.; Frenking, G. *Chem. - Eur. J.* **2009**, *15*, 3448. (f) Takagi, N.; Shimizu, T.; Frenking, G. *Chem. - Eur. J.* **2009**, *15*, 8593. (g) Takagi, N.; Tonner, R.; Frenking, G. *Chem. - Eur. J.* **2012**, *18*, 1772.
- (a) Mondal, K. C.; Roesky, H. W.; Schwarzer, M. C.; Frenking, G.; Niepötter, B.; Wolf, H.; Herbst-Irmer, R.; Stalke, D. *Angew. Chem., Int. Ed.* **2013**, *52*, 2963. (b) Xiong, Y.; Yao, S.; Tan, G.; Inoue, S.; Driess, M. *J. Am. Chem. Soc.* **2013**, *135*, 5004. (c) Ishida, S.; Iwamoto, T.; Kabuto, C.; Kira, M. *Nature* **2003**, *421*, 725. (d) Kira, M. *Chem. Commun.* **2010**, *46*, 2893. (e) Kira, M.; Iwamoto, T.; Ishida, S.; Masuda, H.; Abe, T.; Kabuto, C. *J. Am. Chem. Soc.* **2009**, *131*, 17135. (f) Iwamoto, T.; Masuda, H.; Kabuto, C.; Kira, M. *Organometallics*

2005, 24, 197. (f) Xiong, Y.; Yao, S.; Inoue, S.; Epping, J. D.; Driess, M. *Angew. Chem., Int. Ed.* **2013**, *52*, 7147.

(9) As recent examples see: (a) Tan, G.; Enthaler, S.; Inoue, S.; Blom, B.; Driess, M. *Angew. Chem., Int. Ed.* **2015**, *54*, 2214. (b) Blom, B.; Pohl, M.; Gallego, D.; Tan, G.; Driess, M. *Organometallics* **2014**, *33*, 5272. (c) Tan, G.; Blom, B.; Gallego, D.; Driess, M. *Organometallics* **2014**, *33*, 363. (d) Gallego, D.; Brück, A.; Irran, E.; Meier, F.; Kaupp, M.; Driess, M.; Hartwig, J. F. *J. Am. Chem. Soc.* **2013**, *135*, 15617. (e) Blom, B.; Enthaler, S.; Inoue, S.; Irran, E.; Driess, M. *J. Am. Chem. Soc.* **2013**, *135*, 6703. (f) Stoelzel, M.; Präsang, C.; Blom, B.; Driess, M. *Aust. J. Chem.* **2013**, *66*, 1163. (g) Brück, A.; Gallego, D.; Wang, W.; Irran, E.; Driess, M.; Hartwig, J. F. *Angew. Chem., Int. Ed.* **2012**, *51*, 11478. (h) Blom, B.; Driess, M.; Gallego, D.; Inoue, S. *Chem. - Eur. J.* **2012**, *18*, 13355. (i) Wang, W.; Inoue, S.; Enthaler, S.; Driess, M. *Angew. Chem., Int. Ed.* **2012**, *51*, 6167. (j) Wang, W.; Inoue, S.; Irran, E.; Driess, M. *Angew. Chem., Int. Ed.* **2012**, *51*, 3691. (k) Stoelzel, M.; Präsang, C.; Inoue, S.; Enthaler, S.; Driess, M. *Angew. Chem., Int. Ed.* **2012**, *51*, 399.

(10) Blom, B.; Klatt, G.; Gallego, D.; Tan, G.; Driess, M. *Dalton Trans.* **2015**, *44*, 639.

(11) (a) Bader, R. F. W. *Chem. Rev.* **1991**, *91*, 893. (b) Bader, R. F. W.; Essen, H. J. *Chem. Phys.* **1984**, *80*, 1943.

(12) Wiberg, K. A. *Tetrahedron* **1968**, *24*, 1083.

(13) See for examples ref 9e and 9h.

(14) Burns, C. J.; Andersen, R. A. *J. Organomet. Chem.* **1987**, *325*, 31.

(15) Surprisingly complex 5-OEt_2 has escaped characterization by single-crystal X-ray diffraction analysis, despite being known since 1987. Since we fortuitously obtained suitable crystals thereof, we carried out such an investigation. Complex 5-OEt_2 features bent Cp* groups, which is typical and unremarkable for complexes of the type $[(\eta^5\text{-C}_5\text{Me}_5)_2\text{Ae}\leftarrow\text{L}]$ (Ae = Ca, Sr, Ba; L = neutral ligand), with the OEt₂ moiety occupying one of the coordination sites. The complex features a Sr–O bond length of 2.5598(14) Å, and the distance from one of the H atoms (H20a) of the methyl group is in close proximity to the Sr center (2.885 Å, dotted line, Figure S14), compared with the other methyl H atoms. This shorter bond distance might be indicative of an agostic interaction to the Sr center (see Figure S12 in the Supporting Information).

(16) Agostic interactions are known for alkaline earth metal complexes. As a recent example, see: Sarazin, Y.; Roşca, D.; Poirier, V.; Roisnel, T.; Silvestru, A.; Maron, L.; Carpentier, J. – F. *Organometallics* **2010**, *29*, 6569.

(17) For an explanation on how measuring frequency affects the NMR time scale see: Bryant, R. G. *J. Chem. Educ.* **1983**, *60*, 933.10.1021/ed060p933

(18) See ref 14: A detectable exchange process is also observed for the PEt₃ analogues.

(19) Teng, W.; Ruhlandt-Senge, K. *Organometallics* **2004**, *23*, 952.

(20) Rieckhoff, M.; Pieper, U.; Stalke, D.; Edelman, F. T. *Angew. Chem.* **1993**, *105*, 1102.

(21) Teng, W.; Ruhlandt-Senge, K. *Organometallics* **2004**, *23*, 2694.

(22) Pyykkö, P.; Atsumi, M. *Chem. - Eur. J.* **2009**, *15*, 186.

(23) Kazhdan, D.; Hu, Y.-J.; Kokai, A.; Levi, Z.; Rozenel, S. *Acta Crystallogr., Sect. E: Struct. Rep. Online* **2008**, *E64*, 1134.

(24) (a) Gans-Eichler, T.; Gudat, D.; Nättinen, K.; Nieger, M. *Chem. - Eur. J.* **2006**, *12*, 1162. (b) Gans-Eichler, T.; Gudat, D.; Nieger, M. *Angew. Chem., Int. Ed.* **2002**, *41*, 1888.

(25) Samples of Cp*₂Ae←:E(N^tBuCH)₂ were tested against decomposition with O₂ and H₂O, respectively, in control experiments to exclude the possibility that the formation of the diazabutadiene complexes is due to decomposition by O₂ or H₂O. In both cases (O₂ or H₂O addition), a color change to yellow is observed along with decomposition to an intractable array of products; however, none of these correspond with the 1,4-diazabuta-1,3-diene Ae complexes 10–12. This rules out that the decomposition is triggered by trace amounts of O₂ or H₂O.

(26) von Schnering, H. G.; Schwarz, M.; Nesper, R. *J. Less-Common Met.* **1988**, *137*, 297.

(27) Zeilinger, M.; Jantke, L.-A.; Scherf, L. M.; Kiefer, F. G.; Neubüser, G.; Kienle, L.; Karttunen, A. J.; Konar, S.; Häussermann, U.; Fässler, T. F. *Chem. Mater.* **2014**, *26*, 6603.

(28) Conesa, J. C. *J. Phys. Chem. B* **2002**, *106*, 3402.

(29) (a) Kasper, J. S.; Richards, S. M. *Acta Crystallogr.* **1964**, *17*, 752.

(b) Bundy, F. P.; Kasper, J. S. *Science* **1963**, *139*, 340.

(30) Joannopoulos, J. D.; Cohen, M. L. *Phys. Rev. B: Solid State* **1973**, *7*, 2644.

(31) Szczech, J. R.; Jin, S. *Energy Environ. Sci.* **2011**, *4*, 56.

(32) Okamoto, H.; Sugiyama, Y.; Nakano, H. *Chem. - Eur. J.* **2011**, *17*, 9864.